Inorganic polyphosphate potentiates lipopolysaccharide-induced macrophage inflammatory response

Received for publication, November 3, 2019, and in revised form, February 3, 2020 Published, Papers in Press, February 10, 2020, DOI 10.1074/jbc.RA119.011763

Toru Ito[‡], Suguru Yamamoto[‡1], Keiichi Yamaguchi[§], Mami Sato[‡], Yoshikatsu Kaneko[‡], Shin Goto[‡], Yuji Goto[§], and Ichiei Narita[‡]

From the [‡]Division of Clinical Nephrology and Rheumatology, Niigata University Graduate School of Medical and Dental Sciences, 1-757 Asahimachi-dori, Niigata 951-8510, Japan and the [§]Institute for Protein Research, Osaka University, Yamadaoka 3-2, Suita, Osaka 565-0871, Japan

Edited by Dennis R. Voelker

Inorganic polyphosphate (polyP) is a linear polymer of orthophosphate units that are linked by phosphoanhydride bonds and is involved in various pathophysiological processes. However, the role of polyP in immune cell dysfunction is not well-understood. In this study, using several biochemical and cell biology approaches, including cytokine assays, immunofluorescence microscopy, receptor-binding assays with quartz crystal microbalance, and dynamic light scanning, we investigated the effect of polyP on *in vitro* lipopolysaccharide (LPS)-induced macrophage inflammatory response. PolyP up-regulated LPS-induced production of the inflammatory cytokines, such as tumor necrosis factor α, interleukin-1β, and interleukin-6, in macrophages, and the effect was polyP dose– and chain length–dependent. However, orthophosphate did not exhibit this effect. PolyP enhanced the LPS-induced intracellular macrophage inflammatory signals. Affinity analysis revealed that polyP interacts with LPS, inducing formation of small micelles, and the polyP-LPS complex enhanced the binding affinity of LPS to Toll-like receptor 4 (TLR4) on macrophages. These results suggest that inorganic polyP plays a critical role in promoting inflammatory response by enhancing the interaction between LPS and TLR4 in macrophages.

Inorganic polyphosphate (polyP)[2] is a linear polymer of orthophosphate units that are linked by phosphoanhydride bonds, similar to ATP (1). PolyP is ubiquitously found in all living cells, from microorganisms to mammals, and its chain length varies from less than 10 to hundreds of phosphate units (2). In humans, polyP, containing 60–100 phosphate units, is stored in platelet granules and can be released into circulation upon its activation or other physiological stimuli (3). Recent studies have revealed that polyP exhibits various physiological effects, such as activating blood procoagulant cascades (4), eliciting pro-inflammatory response in endothelial cells (5, 6), and promoting amyloid fibril formation (7, 8), and it is possible that the reaction of polyP with inflammatory immune cells is associated with the pathology of infection (6, 9, 10).

Lipopolysaccharide (LPS) is a major component of the outer membrane of Gram-negative bacteria and is one of the primary endotoxins released by these organisms (11). LPS induces an inflammatory response in immunocompetent cells in human and mouse models (12, 13), and it is associated with the incidence of both acute and chronic inflammatory diseases. Toll-like receptor 4 (TLR4) is an LPS receptor expressed on immune cells such as monocytes, macrophages, and granulocytes (12), and activation of TLR4-associated signaling, including mitogen-activated protein kinase (MAPK) and nuclear factor (NF)-κB pathways, induces synthesis of inflammatory cytokines, such as tumor necrosis factor α (TNFα), interleukin (IL)-1β, and IL-6 (13). However, the relation of LPS with polyP in the inflammatory response in immune cells is largely unknown. In this study, we investigated the effects of polyP on LPS-induced inflammatory response in macrophages, focusing on the reaction between polyP and LPS *in vitro*.

Results

PolyP amplified LPS-induced inflammatory response in macrophages

To investigate the effect of polyP on LPS-induced macrophage inflammatory response, THP-1–derived macrophages were reacted with LPS isolated from *Escherichia coli* with or without polyP-65 (chain length 60–70-mer). LPS induced the expression of inflammatory cytokine genes TNFα, IL-1β, and IL-6 in macrophages, as reported previously (14). The addition of polyP-65 markedly enhanced cytokine expression (TNFα: polyP and LPS (7.16 $\pm$ 1.98) *versus* LPS alone (1.14 $\pm$ 0.55); IL-1β: polyP and LPS (5.70 $\pm$ 1.49) *versus* LPS alone (1.38 $\pm$ 0.22); IL-6: polyP and LPS (16.11 $\pm$ 8.63) *versus* LPS alone (0.92 $\pm$ 0.60), $p < 0.05$), whereas polyP-65 itself did not induce macrophage inflammatory response in the absence of LPS (Fig. 1, *A–C*). Consistent with gene expression, polyP-65 greatly amplified the production of cytokines from macrophages in a dose-dependent manner (Fig. 1, *D–F*). The LPS-induced

The authors declare that they have no conflicts of interest with the contents of this article.

This article contains Figs. S1–S6.

[1] To whom correspondence should be addressed. Tel.: 81-25-227-2200; Fax: 81-25-227-0775; E-mail: yamamots@med.niigata-u.ac.jp.

[2] The abbreviations used are: polyP, polyphosphate; LPS, lipopolysaccharide; TLR4, Toll-like receptor 4; TNFα, tumor necrosis factor α; MAPK, mitogen-activated protein kinase; NF, nuclear factor; IL, interleukin; QCM, quartz crystal microbalance; D_h, hydrodynamic diameter; DLS, dynamic light scattering; ITC, isothermal titration calorimetry; A.U., arbitrary units; MD-2, myeloid differentiation protein-2; JNK, c-Jun N-terminal kinase; SAPK, stress-activated protein kinase; HRP, horseradish peroxidase; FBS, fetal bovine serum; GAPDH, glyceraldehyde-3-phosphate dehydrogenase; TBS, Tris-buffered saline; DAPI, 4′,6-diamidino-2-phenylindole; ANOVA, analysis of variance.

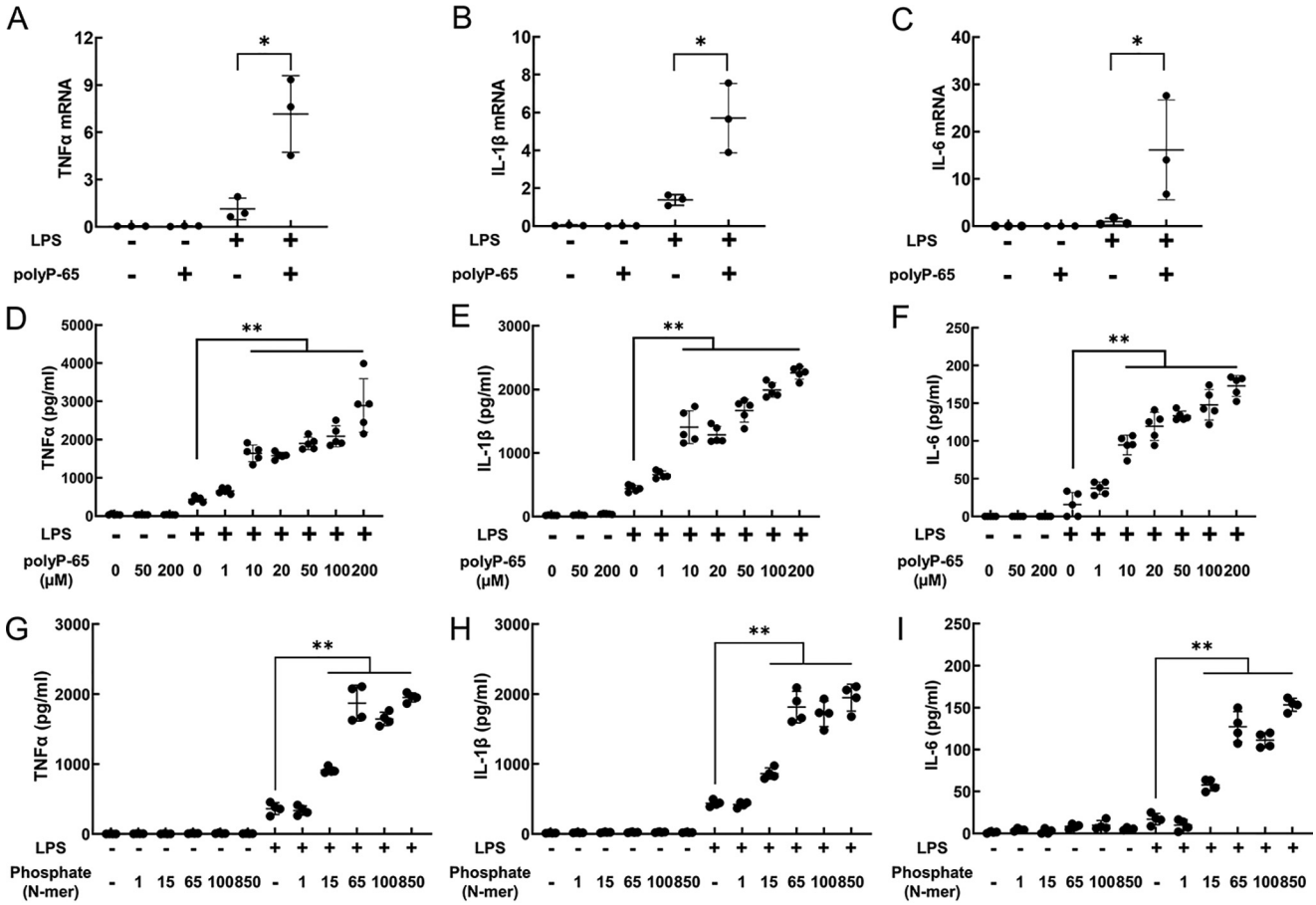

Figure 1. PolyP amplifies LPS-macrophage inflammatory response in THP-1–derived macrophages. *A–I*, cells were incubated with polyP-65 (50 μM) and/or LPS (1.0 ng/ml) for 6 h. TNFα (*A*), IL-1β (*B*), and IL-6 (*C*) mRNA expression was measured and normalized against GAPDH expression. The concentration of TNFα (*D*), IL-1β (*E*), and IL-6 (*F*) was measured in cell supernatants after incubation with varying doses of polyP-65 (0–200 μM) and/or LPS (1.0 ng/ml) for 24 h. The concentration of TNFα (*G*), IL-1β (*H*), and IL-6 (*I*) was measured in cell supernatants after incubation with polyP (0–850-mer, 50 μM) and/or LPS (1.0 ng/ml) for 24 h. Data are shown as the mean ± S.D. (*error bars*) of 3–5 independent experiments. *, $p < 0.05$; **, $p < 0.01$.

macrophage inflammatory cytokine production was also enhanced in a chain length–dependent manner within a range of 1–850 mer (Fig. 1, *G–I*). PolyP did not involve in cell viability in the reaction setting (Fig. S1). Cytokine production was also increased in human peripheral blood mononuclear cells and J774.1 murine macrophages (Fig. S2). These results indicate that polyP amplified LPS-induced macrophage inflammatory response in a dose– and chain length–dependent manner.

PolyP amplified macrophage inflammatory response via downstream signaling of TLR4

To examine the mechanism of polyP-mediated amplification of LPS-induced macrophage inflammatory response, intracellular signaling molecules related to inflammatory response were assessed. PolyP did not change the mRNA expression of TLR4 and the components of the complex, such as CD14 and myeloid differentiation protein-2 (MD-2) in THP-1 cells reacted with LPS (Fig. S3). LPS induced phosphorylation of JNK, NF-κB, and IκBα, but not p38, Erk1/2-MAPK. The phosphorylation was enhanced with the addition of polyP-65 (Fig. 2, *A–E*). In contrast, polyP-65 alone did not affect phosphorylation of these proteins. Furthermore, polyP-65 amplified LPS-induced NLRP3 protein expression in macrophages (Fig. 2*F*). These results suggest that polyP enhances LPS-induced MAPK, NF-κB, and NLRP3 activation in macrophages.

To elucidate the mechanism of polyP-mediated enhancement of LPS-induced activation of downstream signaling of TRL4 in macrophages, we performed experiments using a receptor and a signal blocker associated with LPS. Both TAK242, an antagonist of TLR4, and BAY11-7082, an inhibitor of NF-κB, significantly inhibited the synergistic effect of polyP on LPS-induced cytokine synthesis (Fig. 3, *A–F*).

PolyP promoted binding of LPS with TLR4 on macrophages

To investigate the molecular interactions among polyP, LPS, and TLR4 on macrophages, we used immunofluorescent microscopy, flow cytometry, and quartz crystal microbalance (QCM) analysis. When macrophages were incubated with biotinylated LPS, several dot signals emerged on the surface of cells, and polyP-65 enhanced biotinylated LPS staining on the surface of macrophages (fluorescence intensity: polyP with LPS (213.8 ± 55.7 A.U.) *versus* LPS alone (11.7 ± 6.3 A.U.), $p < 0.01$) (Fig. 4, *A* and *B*). Flow cytometry analysis showed that treatment with polyP significantly increased the abundance of LPS-FITC–positive macrophages compared with those treated with LPS alone (mean intensity: polyP with LPS (45.62 ± 1.07 A.U.)

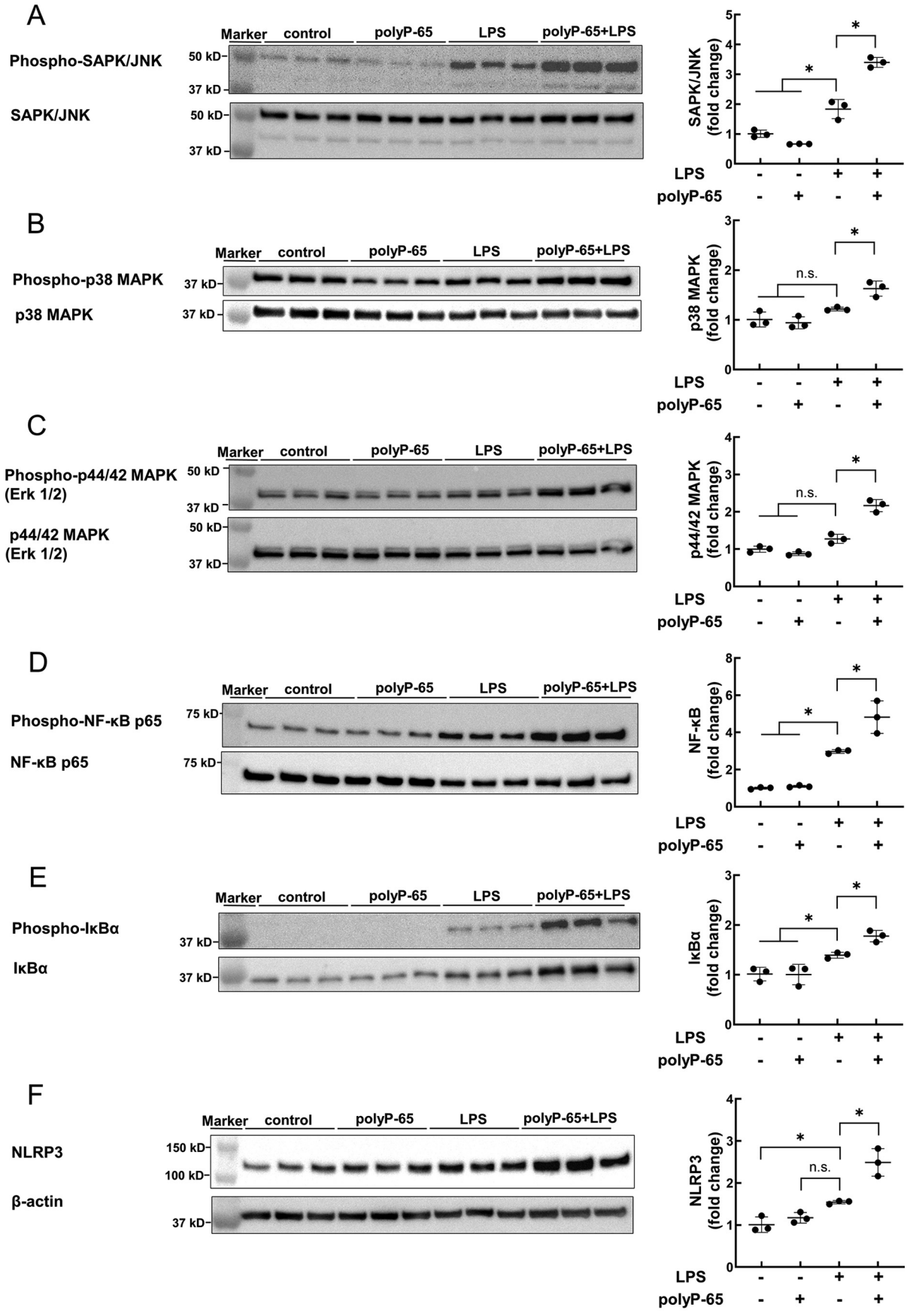

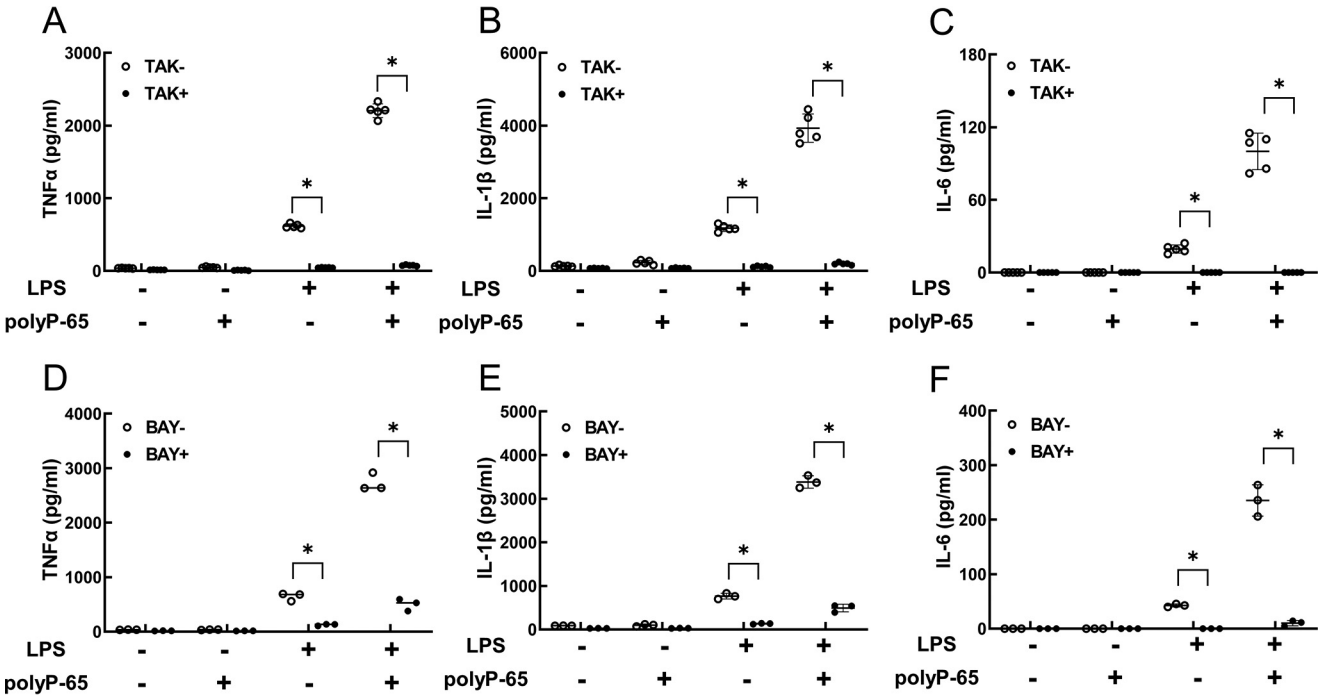

Figure 3. TLR4 antagonist and NF-κB inhibitor inhibited the effect of polyP on enhancement of LPS-induced macrophage inflammatory responses. *A–F*, after 1 h of pretreatment with TLR4 antagonist (TAK242, 10 μM) or NF-κB inhibitor (BAY11-7082, 1.0 μM), cells were incubated with polyP-65 (50 μM) and LPS (1.0 ng/ml) for 24 h. The concentration of TNFα (*A* and *D*), IL-1β (*B* and *E*), and IL-6 (*E* and *F*) was measured in cell supernatants. Data are shown as mean ± S.D. (*error bars*) of three independent experiments. Statistical significance was analyzed by one-way ANOVA followed by Bonferroni post hoc test. *, $p < 0.01$.

versus LPS alone (26.11 ± 0.36 A.U.), $p < 0.01$) (Fig. 4, *C* and *D*). Furthermore, to assess the effect of polyP on the interaction between LPS and TLR4, we performed QCM analysis (Fig. 4, *E–J*). A decrease in resonance frequency was observed when LPS was injected onto a sensor chip containing immobilized TLR4 (Fig. 4*G*). In this system, injection of polyP-65 plus LPS led to a higher reduction in the frequency than was observed after injection of LPS alone (Fig. 4, *H–J*), whereas injection of polyP-65 or buffer alone did not change the frequency (Fig. 4, *E* and *F*). To calculate the kinetic parameter, repetitive injection of LPS and polyP-65 was performed. The amount of change in frequency for each injection was greater in LPS with polyP-65 than in polyP-65 alone. (Fig. S4). The K_D values of LPS to TLR4 were 2.07 μM (LPS) and 1.51 μM (LPS + polyP-65), respectively. We also examined the effect of polyP on the interaction between LPS and other TLR4 complexes, such as CD14 and MD-2, while there was no interaction with LPS (Fig. S5). These results indicate that polyP enhances the interaction between LPS and TLR4 on macrophages.

Interaction between polyP and LPS promoted the formation of smaller LPS micelles

To obtain additional information on the interaction between polyP and LPS, we measured the hydrodynamic diameter (D_h) of LPS micelles in the presence of varying concentrations of polyP-65 using dynamic light scattering (DLS) (Fig. 5*A*). A previous study indicated that LPS forms distinct types of micelles, depending on the concentrations (15); specifically, premicelle oligomers and large aggregates were formed below and above, respectively, the apparent critical micelle concentration of 14 μg/ml LPS. The DLS measurement of LPS micelles in the absence of polyP-65 detected two primary components: component 1 at a D_h value of 26.4 nm and component 2 at a D_h value of 60.6 nm (Fig. 5*A*, 0 μM polyP-65). The fraction of component 1 increased and that of component 2 decreased following treatment with polyP-65 at concentrations higher than 2 μM (Fig. 5*B*). The D_h value of component 1 slightly decreased, but the D_h value of component 2 only slightly changed following treatment with polyP-65 (Fig. 5*C*). PolyP-65 alone did not show measurable scattering intensity at concentrations below 20 μM (data not shown). The interaction between the LPS micelle and polyP-65 shows that polyP-65 destabilizes the larger micelles and increases the proportion of smaller LPS micelles.

To examine the affinity between polyP and LPS, we performed isothermal titration calorimetry (ITC) experiments. The titration of polyP-65 with LPS showed endothermic heat, with a stronger interaction at 25 °C than at 37 °C (Fig. 5*D*). As a control, endothermic heat was not observed with LPS alone (Fig. S6*A*) or polyP-65 alone (Fig. S6*B*). We then analyzed the saturating titration curve at 25 °C (Fig. 5*E*). Parameters could not be assessed at 37 °C owing to poor curve fitting. The

Figure 2. PolyP amplified macrophage inflammatory response via downstream signaling of TLR4. *A–E*, cells were incubated with polyP-65 (50 μM) or LPS (1. 0 ng/ml) alone or in combination for 6 h, and Western blotting was performed on whole-cell lysates to detect signaling proteins. The expression of phosphorylated and total JNK MAPK (*A*), phosphorylated and total p38 MAPK (*B*), phosphorylated and total Erk1/2 MAPK (*C*), phosphorylated and total NF-κB (*D*), phosphorylated and total IκBα (*E*), and NLRP3 (*F*) in THP-1–derived macrophages was analyzed by Western blotting (*left*) and quantified by densitometric analysis normalized against total protein (*right*). β-Actin was used as a loading control. Data are shown as mean ± S.D. (*error bars*) of three independent experiments. Statistical significance was analyzed by one-way ANOVA followed by Bonferroni post hoc test. *, $p < 0.01$; *n.s.*, not significant.

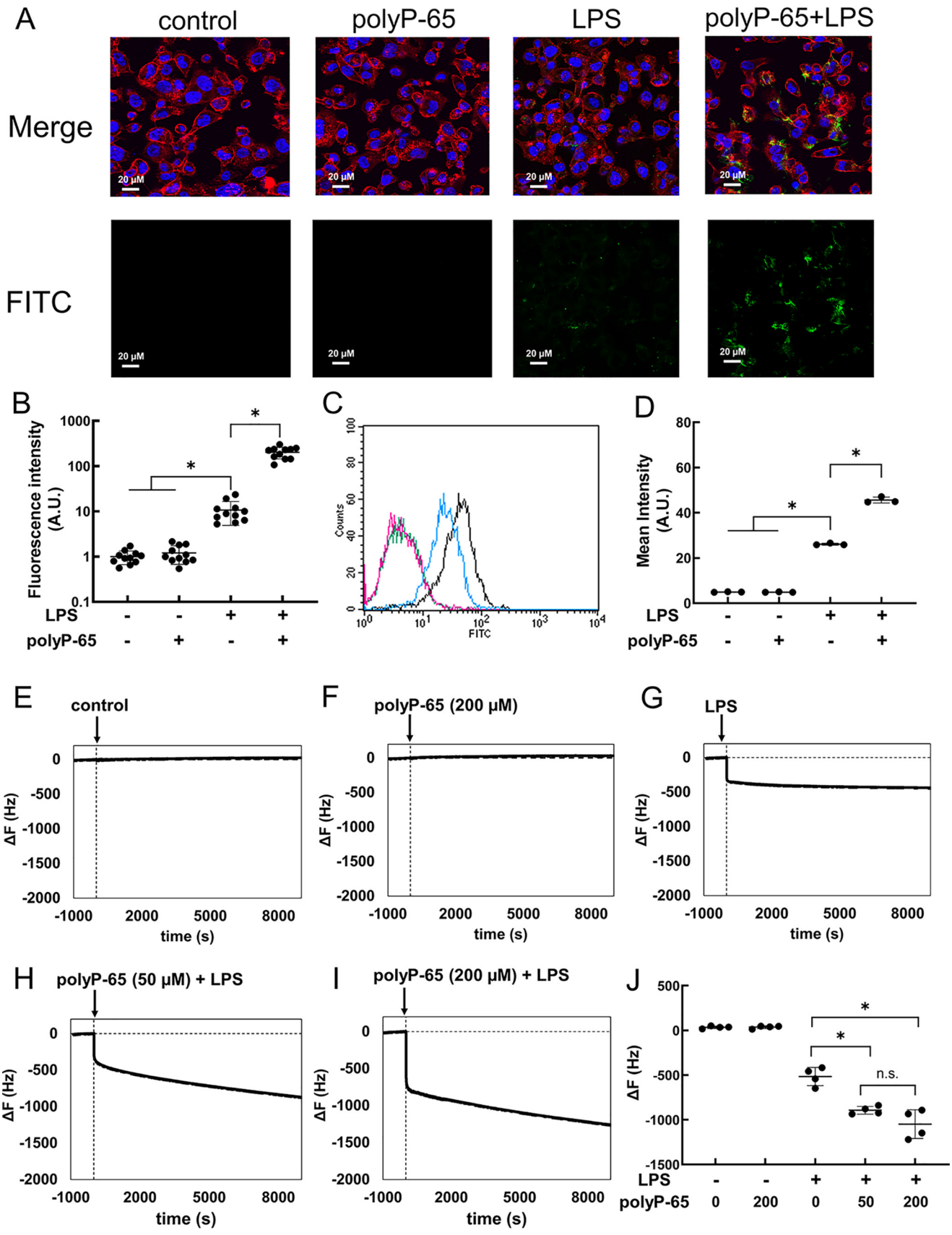

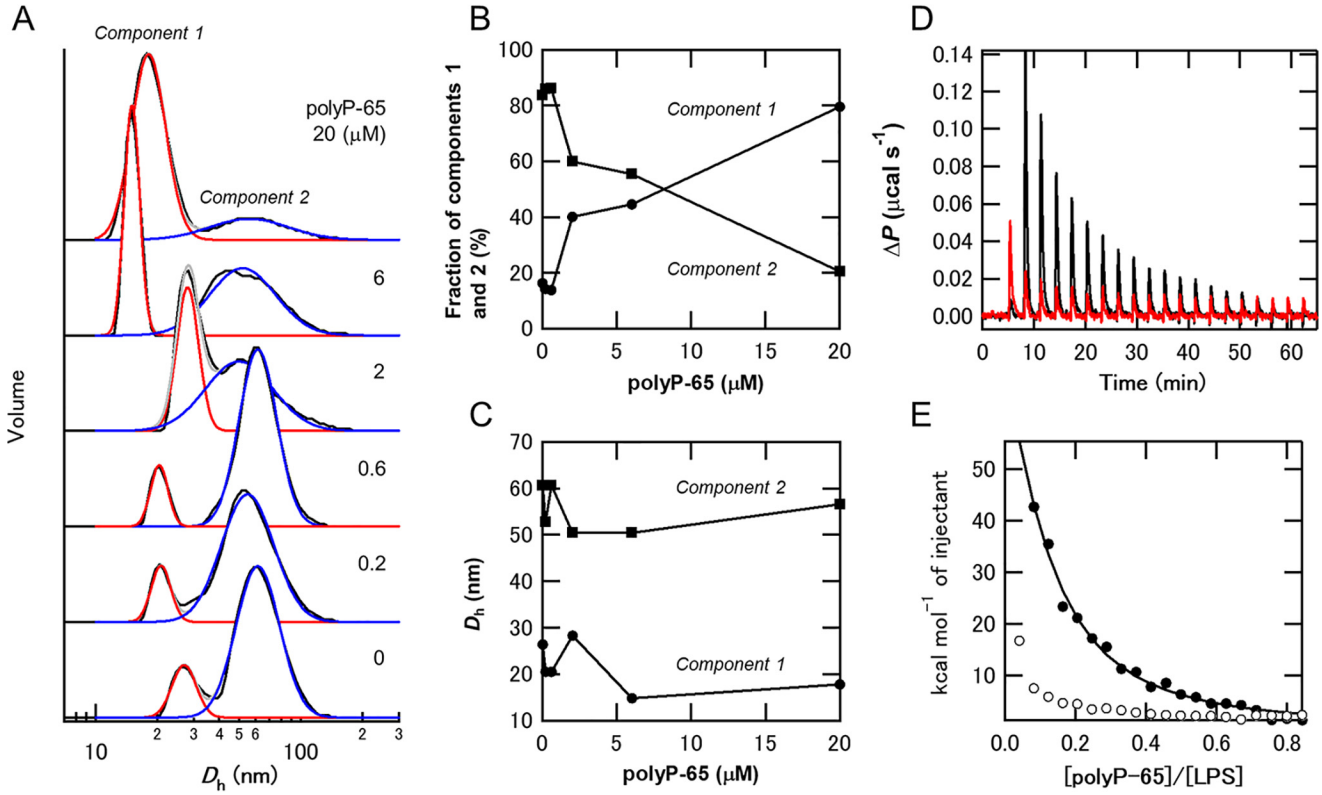

Figure 5. Interaction between polyP and LPS promoted the formation of smaller LPS micelles. *A*, hydrodynamic diameter (D_h) of LPS micelles in the presence of varying concentrations of polyP-65 (*black*). Component 1 (*red*) and component 2 (*blue*) were estimated by fitting the D_h values obtained experimentally with Gaussian curves. The fitted curves consisting of the sum of components 1 and 2 are shown in *gray lines*. The concentration of polyP-65 is noted in the figure. Shown are the fraction (*B*) and the D_h (*C*) of components 1 (*circles*) and 2 (*squares*) obtained from Gaussian fitting. *D*, direct heat effects for the injection of polyP-65 into 0.01 mg/ml LPS at 25 °C (*black*) and 37 °C (*red*). *E*, total heat effects for each injection at 25 °C (*closed circles*) and 37 °C (*open circles*) at an LPS concentration of 1.67 μM. The concentration of LPS was estimated by assuming the molecular weight of LPS to be 6,000. The curve fitting was performed only at 25 °C (*black lines*).

apparent stoichiometry of binding was as follows: 1 mol of LPS interacted with 0.036–0.072 mol of polyP-65 (14–28 mol of LPS interacted with 1 mol of polyP-65) when the molecular weight of LPS was assumed to be in the range of 3,000–6,000, with a K_d of 0.26 ± 0.05 μM. The ΔH, $-T\Delta S$, and ΔG values for binding were 199 ± 111, −208, and −8.81 kcal/mol, respectively. Thermodynamic parameters indicated that the driving force for favorable ΔG arises from the positive entropy change (ΔS). These results suggest that polyP-65 interacts with LPS micelles consisting of 14–28 molecules, leading to a net dehydration (*i.e.* removal of water molecules) around polyP-65 or LPS micelles, and converts the large micelles into smaller micelles.

Discussion

In this study, we report that inorganic polyP amplified LPS-induced macrophage inflammatory response *in vitro* by enhancing the binding affinity of LPS to TLR4 and promoting LPS micelle formation.

Several studies have shown the role of polyP in inflammation and blood clotting cascades. For example, polyP amplifies the inflammatory response of nuclear proteins in human umbilical vein endothelial cells by enhancing multiple ligand-receptor signaling pathways (6, 10). In our study, polyP significantly enhanced LPS-induced cytokine production in macrophages in a dose– and chain length–dependent manner (Fig. 1). In this experimental system, monophosphate did not promote macrophage inflammation, suggesting that polymerization of phosphate could be crucial for the reaction. The effect of polyP on LPS-induced macrophage inflammation was more prominent when the chain length was greater than 65 monomers (Fig. 1, *G–I*). Middle-length chain polyP (60–100-mer) is known to be stored in platelets and released into circulation during systemic

Figure 4. PolyP promoted binding of LPS to TLR4 on macrophages. *A*, cells were treated with biotinylated LPS (1.0 μg/ml) and/or polyP-65 (50 μM) for 3 h. LPS attached to the cell membrane was detected using a FITC-labeled anti-biotin antibody (*green*). Cells were stained with DAPI (*blue*) and rhodamine phalloidin (*red*) to visualize nuclei and F-actin, respectively. *B*, densitometric analysis of FITC signal to quantify biotinylated LPS attached to cells. The results are shown as mean ± S.D. (*error bars*). Data were analyzed by one-way ANOVA followed by Bonferroni post hoc test. *, $p < 0.01$. *C*, flow cytometric analysis was performed to quantify LPS attached to cells treated with biotinylated LPS (1.0 μg/ml) and/or polyP-65 (50 μM) for 3 h. Representative data show *green*, *pink*, *blue*, and *black* as control, polyP-65, LPS, and polyP-65 + LPS groups, respectively. *D*, quantitative analysis of the geometric mean fluorescence intensities for FITC. Data were analyzed by one-way ANOVA followed by Bonferroni post hoc test. *, $p < 0.01$. *E–I*, QCM analysis to reveal the effect of polyP on LPS binding to TLR4. PolyP-65 (50 or 200 μM) with or without LPS (1.0 μg/ml) was injected into the chamber containing a sensor tip immobilized with recombinant TLR4. The binding of LPS to TLR4 was indicated by a change in the frequency from zero position (ΔF). Samples were injected at the time point indicated by the *arrow*. Representative data are shown. *J*, ΔF at the time point of 10,000 s from injection was measured as mean ± S.D. of three independent experiments. Statistical significance was analyzed by one-way ANOVA followed by Bonferroni post hoc test. *, $p < 0.01$. *n.s.*, not significant.

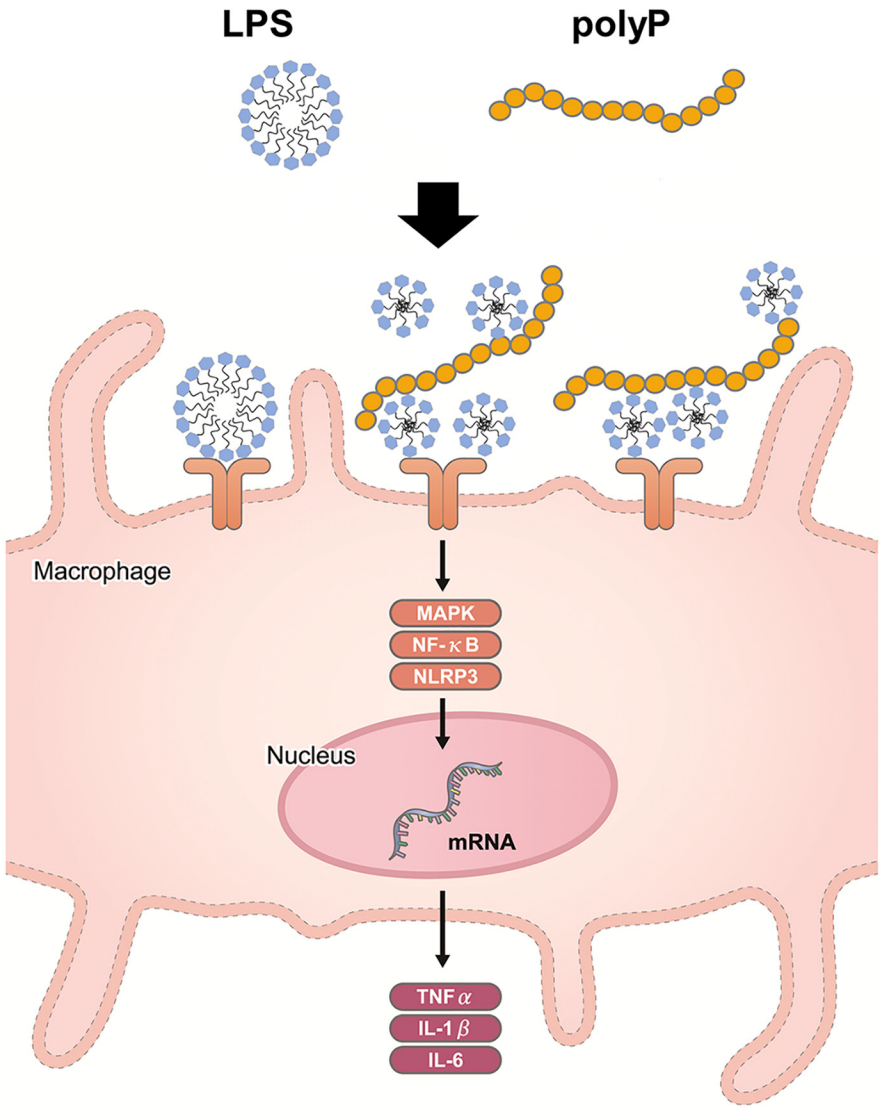

Figure 6. Hypothetical model of polyP for inflammatory response induced by LPS in macrophages. PolyP is released from platelets or bacteria during sepsis. PolyP promotes smaller micelle formation of LPS from bacteria, which facilitates binding to TLR4. The binding of this polyP-LPS complex to TLR4 results in activation of several pro-inflammatory signaling molecules (MAPK, NF-κB, and NLRP3), thereby promoting production of inflammatory cytokines (TNFα, IL-1β, and IL-6).

inflammation (4, 16). Long-chain polyP (greater than several hundred monomers) is synthesized enzymatically and stored in bacteria (17) and is released into circulation during infection (6, 10, 17). Thus, it is possible that circulating middle- and/or long-chain polyP was produced during sepsis and enhanced the reaction between LPS and immune cells.

To understand the detailed mechanism of the effect of polyP on LPS-induced macrophage inflammatory response, we examined the reaction of polyP with LPS, which then reacted with TLR4 on the surface of immune cells. DLS measurements indicated that polyP induced the conversion of larger LPS micelles to smaller micelles in a polyP concentration–dependent manner (Fig. 5*B*). ITC measurements indicated that 14–28 mol of LPS interacted with 1 mol of polyP-65 by an entropy-driven reaction. LPS consists of three components, lipid A, *O*-specific chain, and core oligosaccharide, (11, 15), and has been reported to form micelles (15). Our QCM analysis and immunofluorescence studies (Figs. 4*A* and 5) revealed that the negatively charged polyP enhanced the interaction between TLR4 and LPS that accelerated micelle formation. Previous reports have shown that polyP binds to nuclear cytokines and stabilizes ligand-receptor affinity (6, 10); however, our experimental system showed that polyP enhanced the interaction between LPS and macrophages, but polyP itself did not induce macrophage inflammatory response (Figs. 1–3).

Based on our findings, we proposed a novel hypothesis for the role of polyP in LPS-induced macrophage inflammatory response (Fig. 6). PolyP is stored in serum, plasma, or platelets of individuals. Sepsis induces the release of polyP and LPS from bacteria or activates platelets to release their stored polyP. The released or stored polyP promotes LPS to form smaller micelles, which facilitate binding of LPS to TLR4 on immune cells with higher intensity than in the absence of polyP. Thus, the polyP-LPS complex amplifies the signaling from TLR4 to downstream

molecules, such as MAPK and NF-κB, which enhance inflammatory cytokine production from macrophages. Excess cytokine production driven by polyP may exacerbate systemic inflammatory disease. Our results are limited to *in vitro* experiments, and further research is needed to elucidate the role of polyP and its metabolism in clinical sepsis.

In conclusion, polyP amplified LPS-induced macrophage inflammatory response *in vitro*. PolyP promoted smaller micelle formation by LPS and accelerated the binding of LPS to TLR4 on macrophages. Our findings provide new perspectives and a novel therapeutic target for inflammatory diseases.

Experimental procedures

Reagents and antibodies

PolyP-15 (10–15-mer), polyP-65 (60–70-mer), and polyP-850 (700–1,000-mer) were purchased from Bioenex Inc. (Hiroshima, Japan), and polyP-100 (100-mer) was purchased from Kerafast (Boston, MA). *E. coli* LPS (O111:B4) was purchased from Sigma–Aldrich. NF-κB p65 (C22B4) rabbit mAb, phospho-NF-κB p65 (Ser-536) (93H1) rabbit mAb, SAPK/JNK rabbit mAb, phospho-SAPK/JNK (Thr-183/Tyr-185) (81E11) rabbit mAb, p38 MAPK (D13E1) XP® rabbit mAb, phospho-p38 MAPK (Thr-180/Tyr-182) (D3F9) XP® rabbit mAb, p44/42 MAPK (Erk1/2) (137F5) rabbit mAb, phospho-p44/42 MAPK (Erk1/2) (Thr-202/Tyr-204) (D13.14.4E) XP® rabbit mAb, IκBα (L35A5) mouse mAb, phospho-IκBα (Ser-32/36) (5A5) mouse mAb, NLRP3 (D4D8T) rabbit mAb, goat anti-rabbit IgG reacted with horseradish peroxidase (HRP)-linked antibody, and horse anti-mouse IgG HRP-linked antibody were purchased from Cell Signaling Technology (Danvers, MA). Anti-β-actin Ab-HRP-direct rabbit IgG was purchased from MBL (Aichi, Japan).

Cell culture

THP-1 human monocytic leukemia cells (American Type Culture Collection, Manassas, VA) were cultured in RPMI 1640 (Thermo Fisher Scientific), supplemented with 10% heat-inactivated fetal bovine serum (FBS), penicillin (100 units/ml)/streptomycin (100 μg/ml) (Thermo Fisher Scientific), 10 mM HEPES (Thermo Fisher Scientific), 1× minimum Eagle's medium vitamin (Thermo Fisher Scientific), and 0.5 μM 2-mercaptoethanol. Cells were incubated at 37 °C in humidified air under 5% CO_2. THP-1 cells at a density of 1×10^6 cells/ml were differentiated into macrophages following incubation with 50 ng/ml phorbol 12-myristate 13-acetate (Sigma–Aldrich) for 72 h (THP-1 macrophages). Macrophage differentiation from monocytes was detected by their adherence to the culture plate. Cells were then washed with PBS and replaced with serum-free medium for 24 h before further experiments.

Measurement of mRNA expression

THP-1 macrophages were incubated with LPS (1.0 ng/ml) with or without polyP-65 (50 μM) for 24 h. Total RNA was extracted from cells using the GenElute mammalian total RNA miniprep kit (Sigma–Aldrich) in accordance with the manufacturer's protocols. Quantitative real-time PCR was performed using the One-Step SYBR Plus RT-PCR kit on a thermal cycler Dice real-time system (TP900, Takara, Shiga, Japan). Primers for human TNFα (HA252960, Takara), IL-1β (HA106116, Takara), IL-6 (HA032507, Takara), TLR4 (HA216500, Takara), CD14 (HA154223, Takara), MD-2 (HA160690, Takara), and glyceraldehyde-3-phosphate dehydrogenase (GAPDH) (HA067812, Takara) were used for this analysis. GAPDH was used as an internal control.

In vitro quantification of inflammatory cytokines

THP-1 macrophages were incubated with or without LPS (1.0 ng/ml) and/or 0–200 μM polyP (mono P, polyP-15, polyP-65, polyP-100, and polyP-850) in FBS-free medium for 24 h. Concentrations of these polyPs are expressed in terms of orthophosphate monomers. Cell supernatants were collected, and the concentrations of TNFα, IL-1β, and IL-6 were measured using human TNFα, IL-1β, and IL-6 ELISA kits (R&D Systems, Minneapolis, MN), respectively, according to the manufacturer's protocols.

Detection of proteins in cells

THP-1 macrophages were incubated with or without LPS (1.0 ng/ml) and/or polyP-65 (50 μM) for 6 h. Western blot analysis was performed to detect the phosphorylation of JNK, p38, Erk1/2-MAPK, NF-κB p65, and IκBα and the expression of NLRP3 in cells. Whole-cell lysates were lysed with radioimmune precipitation assay buffer (FUJIFILM Wako, Osaka, Japan), supplemented with protease inhibitor mixture (Roche, Basel, Switzerland) and phosphatase inhibitor mixture (Roche). The lysates were centrifuged at 13,000 × *g* for 20 min at 4 °C, and the protein concentration was evaluated using a BCA protein assay kit (Thermo Fisher Scientific) according to the manufacturer's protocol. The proteins were boiled in SDS sample buffer (TEFCO, Tokyo, Japan) and 10% 2-mercaptoethanol at 95 °C for 5 min. The sample was resolved using 10% SDS-PAGE and transferred to a polyvinylidene fluoride membrane (Atto, Tokyo, Japan). Membranes were blocked with Western Blocking Reagent (Roche), which was diluted with 50 μM Tris-buffered saline (TBS), and incubated with primary antibodies overnight at 4 °C. After washing with TBS containing 0.05% Tween 20, the membranes were incubated with HRP-linked secondary antibodies for 1 h at 20 °C. After incubation with secondary antibodies, signals were visualized as chemiluminescence by ECL Western blotting substrate (Thermo Fisher Scientific) and detected using WSE-6100 LuminoGraph (Atto). Chemiluminescence intensity was calculated using ImageJ software (National Institutes of Health, Bethesda, MD). All antibodies were diluted 1:1,000.

Cell viability assay

To assess the viability of THP-1 macrophages reacted with LPS and polyP-65, we performed a cell viability assay using Cell Counting Kit-8 (CCK-8) (DOJINDO, Kumamoto, Japan) according to the manufacturer's protocol (18).

Reaction with NF-κB inhibitor and TLR4 receptor inhibitor

THP-1 macrophages were incubated with a 1.0 μM concentration of either the NF-κB inhibitor BAY11–7082 (Sigma–Aldrich) or the TLR4 inhibitor TAK-242 (Sigma–Aldrich) for

1 h before incubation with LPS and polyP. After incubation, levels of cytokines in cell supernatant were measured using ELISA kits as described above.

Immunofluorescence microscopy

THP-1 cells were seeded in 8-well culture slides (Corning, Inc., Corning, NY) and differentiated to macrophages as described above. Differentiated cells were incubated with or without 1.0 μg/ml biotinylated LPS (*In vivo* Gen, San Diego, CA) and/or polyP-65 (50 μM) for 3 h. Cells were then washed with PBS and fixed with 4% paraformaldehyde for 20 min. After washing with PBS, cells were incubated with FITC-labeled anti-biotin rabbit polyclonal antibody (Abcam, Cambridge, UK) for 1 h at 20–25 °C (diluted 1:500). After washing with PBS, the cells were incubated with rhodamine phalloidin (Thermo Fisher Scientific) to visualize F-actin. Stained cells were mounted with HardSet Mounting Medium with DAPI (Vector Laboratories, Burlingame, CA). Images were acquired using a FV1200 confocal microscope (Olympus, Tokyo, Japan). The fluorescence intensity was quantified using ImageJ software.

Flow cytometry

THP-1 macrophages were incubated with biotinylated LPS with or without polyP-65 (50 μM) for 3 h. Cells were then washed with PBS and incubated with FITC-labeled anti-biotin rabbit polyclonal antibody for 1 h at room temperature (diluted 1:500). After washing with PBS, cells were collected and washed with FACS buffer (3% FBS and 0.01% sodium azide in PBS). Flow cytometric analysis was performed with FACSCalibur using Cell Quest Pro software (BD Biosciences). Analysis was performed after 10,000 counting events. The mean fluorescence intensity value was used to estimate LPS levels in cells.

Assessing interaction between LPS and TLR4, MD2, and CD14 using QCM

Binding of LPS to TLR4 was assessed using a highly sensitive 27-MHz instrument (AFFINIX Q8, ULVAC, Kanagawa, Japan) as described previously (19). Briefly, QCM sensor chips were prepared using the immobilization kit for AFFINIX (ULVAC) according to the manufacturer's protocol. Recombinant human TLR4 (50 μg/ml), MD2 (50 μg/ml), and CD14 (50 μg/ml) (R&D Systems) were then immobilized on the sensor chip. The sensor chips were soaked in distilled water in the incubation chamber. LPS was injected into the chamber in the presence or absence of polyP-65 for binding to TLR4. The resonance frequency of QCM at equilibrium was defined as the zero position. The stability and drift of the 27-MHz QCM frequency in solution were $\pm$3 Hz. Binding affinity was determined by the frequency change following injection of each sample.

Kinetic analysis between LPS and polyP-65 was performed using repetitive injection of LPS and LPS with polyP-65 as described previously (20). AQUA software (ULVAC) was used to calculate the kinetic parameters.

Dynamic light scanning

DLS measurements were performed with 0.01 mg/ml LPS solutions containing varying concentrations of polyP-65, 10 mM NaP_i (pH 7), and 150 mM NaCl at 37 °C using Zetasizer μV (Malvern Panalytical, Worcestershire, UK). Intensity distribution data were mathematically converted into volume distribution data, which were fitted by Gaussian curves to evaluate the fraction of distinct components.

Isothermal titration calorimetry

ITC measurements were performed using a VP-ITC instrument (MicroCal, Northampton, MA) at neutral pH (H_2O) at 25 °C and 37 °C. Five microliters of 20 μM polyP-65 in a syringe was titrated into 0.01 mg/ml LPS in the ITC cell. For control experiments, 5 μl of 20 μM polyP-65 was titrated into H_2O, or 5 μl of H_2O was titrated into 0.01 mg/ml LPS. During ITC experiments, 20 successive injections were performed 180 s apart, and the cell was continuously stirred at 633 rpm. ITC data were analyzed using Origin software. The thermodynamic parameters were obtained from the integrated heat using a single set of binding sites model.

Statistical analysis

Data were expressed as mean $\pm$ S.D. Statistical analysis was performed by Student's *t* test when only two value sets were compared. One-way analysis of variance (ANOVA) followed by Bonferroni's multiple-comparison test was used to compare three or more groups. The number of biological samples (*n*) for each group and the utilized statistical tests are indicated in the corresponding figure legends. Differences in means were considered statistically significant if $p < 0.05$. No exclusion criteria were incorporated in the design of the experiments for this study.

Author contributions—T. I., S. Y., K. Y., M. S., Y. K., S. G., Y. G., and I. N. conceptualization; T. I., S. Y., K. Y., M. S., Y. K., Y. G., and I. N. data curation; T. I., S. Y., and M. S. formal analysis; T. I., S. Y., K. Y., Y. K., S. G., Y. G., and I. N. investigation; T. I., S. Y., K. Y., M. S., Y. K., S. G., Y. G., and I. N. methodology; T. I., S. Y., and K. Y. writing-original draft; T. I., S. Y., K. Y., Y. K., S. G., Y. G., and I. N. project administration; T. I., S. Y., Y. K., S. G., Y. G., and I. N. writing-review and editing; Y. G. and I. N. funding acquisition.

Acknowledgments—We thank Akiko Seino for technical assistance and Koichi Komochi and Sawako Goto for assistance with QCM analysis.

References

1. Kumble, K. D., and Kornberg, A. (1995) Inorganic polyphosphate in mammalian cells and tissues. *J. Biol. Chem.* **270,** 5818–5822 CrossRef Medline
2. Rao, N. N., Gómez-García, M. R., and Kornberg, A. (2009) Inorganic polyphosphate: essential for growth and survival. *Annu. Rev. Biochem.* **78,** 605–647 CrossRef Medline
3. Ruiz, F. A., Lea, C. R., Oldfield, E., and Docampo, R. (2004) Human platelet dense granules contain polyphosphate and are similar to acidocalcisomes of bacteria and unicellular eukaryotes. *J. Biol. Chem.* **279,** 44250–44257 CrossRef Medline
4. Müller, F., Mutch, N. J., Schenk, W. A., Smith, S. A., Esterl, L., Spronk, H. M., Schmidbauer, S., Gahl, W. A., Morrissey, J. H., and Renné, T. (2009) Platelet polyphosphates are proinflammatory and procoagulant mediators *in vivo*. *Cell* **139,** 1143–1156 CrossRef Medline
5. Bae, J.-S., Lee, W., and Rezaie, A. R. (2012) Polyphosphate elicits pro-inflammatory responses that are counteracted by activated protein C in both cellular and animal models. *J. Thromb. Haemost.* **10,** 1145–1151 CrossRef Medline

6. Dinarvand, P., Hassanian, S. M., Qureshi, S. H., Manithody, C., Eissenberg, J. C., Yang, L., and Rezaie, A. R. (2014) Polyphosphate amplifies proinflammatory responses of nuclear proteins through interaction with receptor for advanced glycation end products and P2Y1 purinergic receptor. *Blood* **123,** 935–945 CrossRef Medline
7. Zhang, C. M., Yamaguchi, K., So, M., Sasahara, K., Ito, T., Yamamoto, S., Narita, I., Kardos, J., Naiki, H., and Goto, Y. (2019) Possible mechanisms of polyphosphate-induced amyloid fibril formation of β_2-microglobulin. *Proc. Natl. Acad. Sci. U.S.A.* **116,** 12833–12838 CrossRef Medline
8. Cremers, C. M., Knoefler, D., Gates, S., Martin, N., Dahl, J.-U., Lempart, J., Xie, L., Chapman, M. R., Galvan, V., Southworth, D. R., and Jakob, U. (2016) Polyphosphate: a conserved modifier of amyloidogenic processes. *Mol. Cell* **63,** 768–780 CrossRef Medline
9. Morrissey, J. H., Choi, S. H., and Smith, S. A. (2012) Polyphosphate: an ancient molecule that links platelets, coagulation, and inflammation. *Blood* **119,** 5972–5979 CrossRef Medline
10. Biswas, I., Panicker, S. R., Cai, X., Mehta-D'souza, P., and Rezaie, A. R. (2018) Inorganic polyphosphate amplifies high mobility group box 1-mediated von Willebrand factor release and platelet string formation on endothelial cells. *Arterioscler. Thromb. Vasc. Biol.* **38,** 1868–1877 CrossRef Medline
11. Dong, H., Xiang, Q., Gu, Y., Wang, Z., Paterson, N. G., Stansfeld, P. J., He, C., Zhang, Y., Wang, W., and Dong, C. (2014) Structural basis for outer membrane lipopolysaccharide insertion. *Nature* **511,** 52–56 CrossRef Medline
12. Vaure, C., and Liu, Y. (2014) A comparative review of toll-like receptor 4 expression and functionality in different animal species. *Front. Immunol.* **5,** 316 Medline
13. Guha, M., and Mackman, N. (2001) LPS induction of gene expression in human monocytes. *Cell. Signal.* **13,** 85–94 CrossRef Medline
14. Schildberger, A., Rossmanith, E., Eichhorn, T., Strassl, K., and Weber, V. (2013) Monocytes, peripheral blood mononuclear cells, and THP-1 cells exhibit different cytokine expression patterns following stimulation with lipopolysaccharide. *Mediators Inflamm.* **2013,** 697972 CrossRef Medline
15. Santos, N. C., Silva, A. C., Castanho, M. A. R. B., Martins-Silva, J., and Saldanha, C. (2003) Evaluation of lipopolysaccharide aggregation by light scattering spectroscopy. *Chembiochem* **4,** 96–100 CrossRef Medline
16. Verhoef, J. J. F., Barendrecht, A. D., Nickel, K. F., Dijkxhoorn, K., Kenne, E., Labberton, L., McCarty, O. J. T., Schiffelers, R., Heijnen, H. F., Hendrickx, A. P., Schellekens, H., Fens, M. H., de Maat, S., Renné, T., and Maas, C. (2017) Polyphosphate nanoparticles on the platelet surface trigger contact system activation. *Blood* **129,** 1707–1717 CrossRef Medline
17. Kornberg, A., Rao, N. N., and Ault-Riché, D. (1999) Inorganic polyphosphate: a molecule of many functions. *Annu. Rev. Biochem.* **68,** 89–125 CrossRef Medline
18. Tominaga, H., Ishiyama, M., Ohseto, F., Sasamoto, K., Hamamoto, T., Suzuki, K., and Watanabe, M. (1999) A water-soluble tetrazolium salt useful for colorimetric cell viability assay. *Anal. Commun.* **36,** 47–50 CrossRef
19. Hori, Y., Aoki, N., Kuwahara, S., Hosojima, M., Kaseda, R., Goto, S., Iida, T., De, S., Kabasawa, H., Kaneko, R., Aoki, H., Tanabe, Y., Kagamu, H., Narita, I., Kikuchi, T., and Saito, A. (2017) Megalin blockade with cilastatin suppresses drug-induced nephrotoxicity. *J. Am. Soc. Nephrol.* **28,** 1783–1791 CrossRef Medline
20. Takakusagi, Y., Kobayashi, S., and Sugawara, F. (2005) Camptothecin binds to a synthetic peptide identified by a T7 phage display screen. *Bioorg. Med. Chem. Lett.* **15,** 4850–4853 CrossRef Medline

Inorganic polyphosphate potentiates lipopolysaccharide-induced macrophage inflammatory response

Toru Ito, Suguru Yamamoto, Keiichi Yamaguchi, Mami Sato, Yoshikatsu Kaneko, Shin Goto, Yuji Goto and Ichiei Narita

J. Biol. Chem. 2020, 295:4014-4023.
doi: 10.1074/jbc.RA119.011763 originally published online February 10, 2020
